JOHANNES GUTENBERG UNIVERSITÄT MAINZ

Calculations of the axial form factor of the nucleon

Alessandro Barone

in collaboration with

D. Djukanovic, G. von Hippel,
H. B. Meyer, K. Ottnad, H. Wittig

KPH Days
6 July 2026, Mainz

Outline

- Introduction and motivation
- Lattice QCD and setup
- Analysis strategy
- Final results

Introduction and motivation

Introduction and motivation

Neutrino-nucleon low-energy scattering dominated by (quasi-)elastic scattering off single nucleon
$\Rightarrow$ need to determine nucleon matrix elements from theory to provide input for experiments

axial form factor

pseudoscalar form factor

$$\langle N(p',s')|\, A_\mu^a(0)\, |N(p,s)\rangle = \bar{U}_N(p',s')\left[\gamma_\mu\gamma_5 \boxed{G_A(Q^2)} - \frac{Q_\mu}{2M_N}\gamma_5 \boxed{G_P(Q^2)}\right]\frac{\lambda^a}{2}\boxed{U_N(p,s)}$$

$SU(3)_f$ spinor
$\lambda_a =$ Gell-Mann matrices

- $G_A(Q^2)$: relevant for neutrino scattering experiments - main source of errors in neutrino-nucleon interactions
- $G_P(Q^2)$: smaller impact on the cross-section, mainly relevant at small Q^2

Nucleon interactions

Different $SU(3)$ flavour combinations play different roles in neutrino-nucleon scattering:

- $A^3_\mu \to G_A^{u-d}(Q^2)$:**isovector** $\to$ sensitive to $W^\pm$ (β decays)
- $\begin{cases} A^8_\mu \to G_A^{u+d-2s}(Q^2) & \textbf{:isoscalar octet} \\ A^0_\mu \to G_A^{u+d+s}(Q^2) & \textbf{:isoscalar singlet} \end{cases}$ $\to$ sensitive to Z^0(elastic scattering)

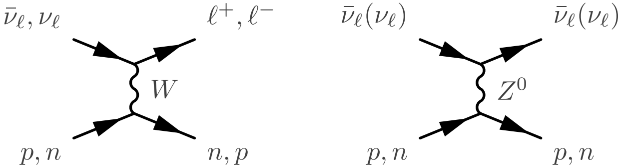

Theoretical input from LQCD

1. isovector well studied and in agreement between collaborations (see a review here [Meyer et al. (2022)[1]]), in slight tension with experiments [Meyer et al. (2016)[2]]
2. isoscalar [Barone et al. (2025)[3], Barone et al. (2026)[4]] and flavour decomposition [Alexandrou et al. (2021)[5]] still need more work

Nucleon structure

All these form factors provide information on the nucleon structure through various quantities

axial charge — axial radius

$$G_A(Q^2) = \boxed{g_A}\left(1 - \frac{1}{6}\boxed{r_A^2}\,Q^2 + \mathcal{O}(Q^4)\right),$$

In particular, the spin S_N can be decomposed [Ji (1997)[6]] as

valence quark angular momentum

$\neq \sum_{q_{\rm val}} S_{q_{\rm val}}$
[Alexakhin et al. (2007)[7]]

$$\boxed{S_N} = \frac{1}{2}\sum_q \boxed{\Delta\Sigma_q} + \sum_{q_{\rm val}} \boxed{L_{q_{\rm val}}} + \boxed{J_g} \longrightarrow \text{gluon angular momentum}$$

intrinsic quark spin $\equiv g_A^q$ $\rightarrow$ include contribution from the sea

All G_A^f are relevant for nucleon structure! MicroBooNE aims to extract [Miceli et al. (2015)[8], Kim et al. (2019)[9]]

$$G_A^s(Q^2)\,, \quad Q^2[\text{GeV}^2] \in [0.08, 1]$$

Axial form factor from LQCD: status from the Mainz group

Lot of efforts in the LQCD Mainz group devoted to and axial nucleon form factor

Isovector axial form factor of the nucleon from lattice QCD

Dalibor Djukanovic,[1,2] Georg von Hippel,[3] Jonna Koponen,[3] Harvey B. Meyer,[1,3] Konstantin Ottnad,[3] Tobias Schulz,[3] and Hartmut Wittig[1,3]

[1]*Helmholtz-Institut Mainz, Johannes Gutenberg-Universität Mainz, D-55099 Mainz, Germany*
[2]*GSI Helmholtzzentrum für Schwerionenforschung, Darmstadt 64291, Germany*
[3]*PRISMA+ Cluster of Excellence & Institut für Kernphysik, Johannes Gutenberg-Universität Mainz, D-55099 Mainz, Germany*

[Djukanovic et al. (2022)[10]]

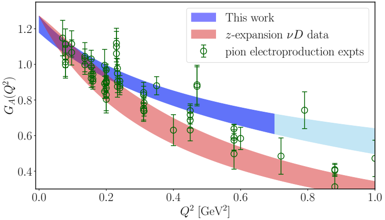

Isoscalar octet axial form factor of the nucleon from lattice QCD

Alessandro Barone,[1,*] Dalibor Djukanovic,[2,3] Georg von Hippel,[1] Jonna Koponen,[1] Harvey B. Meyer,[1,2] Konstantin Ottnad,[1] and Hartmut Wittig[1,2]

[1]*PRISMA+ Cluster of Excellence and Institut für Kernphysik, Johannes Gutenberg-Universität Mainz, D-55099 Mainz, Germany*
[2]*Helmholtz-Institut Mainz, Johannes Gutenberg-Universität Mainz, D-55099 Mainz, Germany*
[3]*GSI Helmholtzzentrum für Schwerionenforschung, 64291 Darmstadt, Germany*

[Barone et al. (2025)[3]]

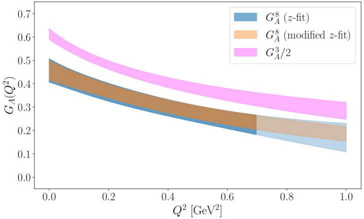

Also efforts in the vector channel, with recent results [Djukanovic et al. (2024)[11], Djukanovic et al. (2024)[12], Djukanovic et al. (2024)[13]]

Axial form factor from LQCD: status from the Mainz group

This talk: summarise strategies and results for all channels based on

The strange and flavor-singlet axial form factors of the nucleon from lattice QCD

Alessandro Barone,[1,*] Dalibor Djukanovic,[2,3] Georg von Hippel,[1]
Harvey B. Meyer,[1,2,4] Konstantin Ottnad,[1,5] and Hartmut Wittig[1,2]
[1] *PRISMA++ Cluster of Excellence & Institut für Kernphysik, Johannes Gutenberg-Universität Mainz, D-55099 Mainz, Germany*
[2] *Helmholtz-Institut Mainz, Johannes Gutenberg-Universität Mainz, D-55099 Mainz, Germany*
[3] *GSI Helmholtzzentrum für Schwerionenforschung, 64291 Darmstadt, Germany*
[4] *Theoretical Physics Department, CERN, 1211 Geneva 23, Switzerland*
[5] *Helmholtz-Institut für Strahlen- und Kernphysik, Universität Bonn, D-53115 Bonn, Germany*

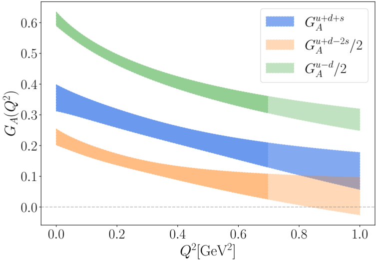

[Barone et al. (2026)[4]]

Lattice QCD and setup

Lattice QCD in 2 slides (1)

We move to Euclidean space through **Wick rotation** $t \to -i\tau$. The path integral becomes

$$\langle \mathcal{O} \rangle = \frac{1}{Z} \int \mathcal{D}[\Phi] \mathcal{O}[\Phi] \, e^{iS_M[\Phi]} \quad \Rightarrow \quad \langle \mathcal{O} \rangle = \frac{1}{Z} \int \mathcal{D}[\Phi] \mathcal{O}[\Phi] \, e^{-S_E[\Phi]}, \quad \Phi = (\bar{\psi}, \psi, U)$$

- Replace continuous **Euclidean spacetime** by a **hypercubic lattice** with volume $V = L^3 \times T$
  $x_\mu = a \, n_\mu \; (n_\mu \in \mathbb{Z})$
  a is the lattice spacing and act as UV cutoff

$$\Lambda_{\mathrm{UV}} \sim \frac{1}{a}$$

- Quark fields $\psi(x)$ live on lattice sites
- Gluon fields $U_\mu(x)$ are represented by link variables connecting neighbouring sites.

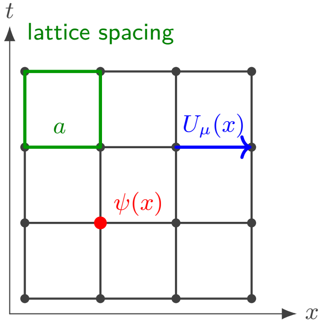

2D sketch of a 4D Euclidean lattice

Lattice QCD in 2 slides (1)

We move to Euclidean space through **Wick rotation** $t \to -i\tau$. The path integral becomes

$$\langle \mathcal{O} \rangle = \frac{1}{Z} \int \mathcal{D}[\Phi]\mathcal{O}[\Phi]\, e^{iS_M[\Phi]} \quad \Rightarrow \quad \langle \mathcal{O} \rangle = \frac{1}{Z} \int \mathcal{D}[\Phi]\mathcal{O}[\Phi]\, e^{-S_E[\Phi]}, \quad \Phi = (\bar{\psi}, \psi, U)$$

- Replace continuous **Euclidean spacetime** by a **hypercubic lattice** with volume $V = L^3 \times T$
  $x_\mu = a\, n_\mu$ $(n_\mu \in \mathbb{Z})$
  a is the lattice spacing and act as UV cutoff

$$\Lambda_{\text{UV}} \sim \frac{1}{a}$$

- Quark fields $\psi(x)$ live on lattice sites
- Gluon fields $U_\mu(x)$ are represented by link variables connecting neighbouring sites.

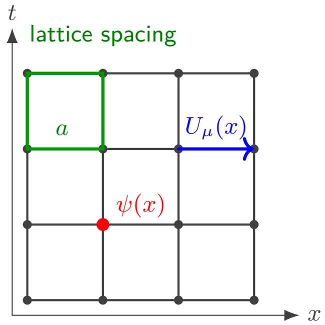

2D sketch of a 4D Euclidean lattice

Lattice QCD in 2 slides (1)

We move to Euclidean space through **Wick rotation** $t \to -i\tau$. The path integral becomes

$$\langle \mathcal{O} \rangle = \frac{1}{Z} \int \mathcal{D}[\Phi]\mathcal{O}[\Phi]\, e^{iS_M[\Phi]} \quad \Rightarrow \quad \langle \mathcal{O} \rangle = \frac{1}{Z} \int \mathcal{D}[\Phi]\mathcal{O}[\Phi]\, e^{-S_E[\Phi]}, \quad \Phi = (\bar{\psi}, \psi, U)$$

- Replace continuous **Euclidean spacetime** by a **hypercubic lattice** with volume $V = L^3 \times T$
  $x_\mu = a\, n_\mu \; (n_\mu \in \mathbb{Z})$
  a is the lattice spacing and act as UV cutoff

$$\Lambda_{\mathrm{UV}} \sim \frac{1}{a}$$

- Quark fields $\psi(x)$ live on lattice sites
- Gluon fields $U_\mu(x)$ are represented by link variables connecting neighbouring sites.

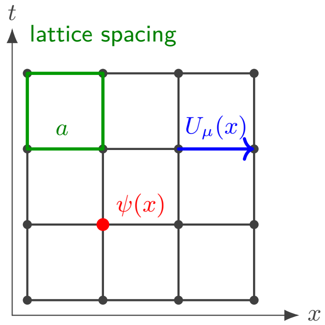

2D sketch of a 4D Euclidean lattice

Lattice QCD in 2 slides (1)

We move to Euclidean space through **Wick rotation** $t \to -i\tau$. The path integral becomes

$$\langle \mathcal{O} \rangle = \frac{1}{Z} \int \mathcal{D}[\Phi]\mathcal{O}[\Phi]\, e^{iS_M[\Phi]} \quad \Rightarrow \quad \langle \mathcal{O} \rangle = \frac{1}{Z} \int \mathcal{D}[\Phi]\mathcal{O}[\Phi]\, e^{-S_E[\Phi]}, \quad \Phi = (\bar{\psi}, \psi, U)$$

- Replace continuous **Euclidean spacetime** by a **hypercubic lattice** with volume $V = L^3 \times T$
  $x_\mu = a\, n_\mu \; (n_\mu \in \mathbb{Z})$
  a is the lattice spacing and act as UV cutoff

$$\Lambda_{\mathrm{UV}} \sim \frac{1}{a}$$

- Quark fields $\psi(x)$ live on lattice sites
- Gluon fields $U_\mu(x)$ are represented by link variables connecting neighbouring sites.

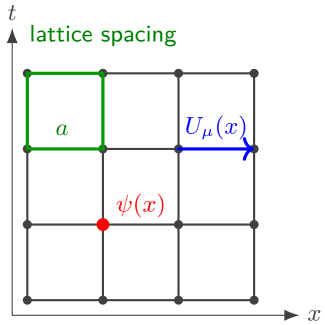

2D sketch of a 4D Euclidean lattice

Lattice QCD in 2 slides (2)

We can then use **Monte Carlo** to evaluate multidimensional integrals by generating a large number of gauge configurations U_α with probability

$$P[U_\alpha] \propto \det[U_\alpha] e^{-S_E[U_\alpha]} \quad \Rightarrow \quad \langle \mathcal{O} \rangle \simeq \frac{1}{N_{\text{config}}} \sum_{\alpha=1}^{N_{\text{config}}} \mathcal{O}[U_\alpha]$$

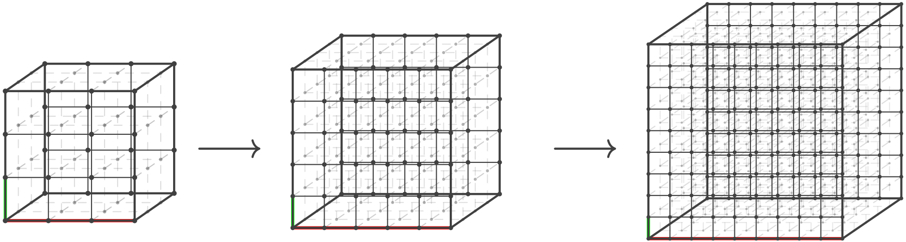

Physical results are recovered by taking the limits (global fit)

$$a \to 0, \qquad L \to \infty, \qquad m_q \to m_q^{\text{phys}} \quad \Rightarrow \quad O(a, L, m_\pi) \longrightarrow O^{\text{phys}}$$

Lattice setup: CLS $N_f = 2 + 1$ ensembles

[Bruno et al. (2015)[17]]

- non-perturbatively $\mathcal{O}(a)$-improved Wilson fermions [Sheikholeslami and Wohlert (1985)[14], Bulava and Schaefer (2013)[15]]
- tree-level improved Lüscher-Weisz gauge action [Luscher and Weisz (1985)[16]]

ID	β	T/a	L/a	M_π [MeV]	$M_\pi L$	M_N [GeV]	N_{conf}	N_{meas}	t_s [fm]	N_{t_s}
H102	3.40	96	32	354	4.96	1.103	2005	32080	0.35..1.47	14
H105	3.40	96	32	280	3.93	1.045	1027	49296	0.35..1.47	14
C101	3.40	96	48	225	4.73	0.980	2000	64000	0.35..1.47	14
N101	3.40	128	48	281	5.91	1.030	1596	51072	0.35..1.47	14
S400	3.46	128	32	350	4.33	1.130	2873	45968	0.31..1.53	9
N451	3.46	128	48	286	5.31	1.045	1011	129408	0.31..1.53	9
D450	3.46	128	64	216	5.35	0.978	500	64000	0.31..1.53	17
N203	3.55	128	48	346	5.41	1.112	1543	24688	0.26..1.41	10
N200	3.55	128	48	281	4.39	1.063	1712	20544	0.26..1.41	10
D200	3.55	128	64	203	4.22	0.966	2000	64000	0.26..1.41	10
E250	3.55	192	96	129	4.04	0.928	400	102400	0.26..1.41	10
N302	3.70	128	48	348	4.22	1.146	2201	35216	0.20..1.40	13
J303	3.70	192	64	260	4.19	1.048	1073	17168	0.20..1.40	13
E300	3.70	192	96	174	4.21	0.962	570	18240	0.20..1.40	13

*We use E300 to demonstrate our approach

Computation strategy on the lattice (1)

The basic quantities computed on the lattice are Euclidean correlation functions, e.g.

$$C^{\Gamma}_{2\mathrm{pt}}(t,\mathbf{p}) = \Gamma_{\alpha\beta}\sum_{\mathbf{x}} e^{-i\mathbf{p}\cdot\mathbf{x}}\langle O_{N,\beta}(\mathbf{x},t)\overline{O}_{N,\alpha}(0)\rangle\,, \quad O_{N,\alpha}(x) = \varepsilon_{abc}\Big(\tilde{u}^T_a(x)C\gamma_5\tilde{d}_b(x)\Big)\tilde{u}_{c,\alpha}(x)$$

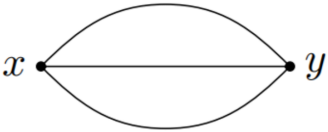

The correlator has the **spectral decomposition**

$$C_{2\mathrm{pt}}(t,\mathbf{p}) = \sum_n |Z_n|^2 e^{-E_n t} \quad \xrightarrow{t\gg 0} \quad |Z_0|^2 e^{-E_0 t}$$

Computation strategy on the lattice (2)

$$C^a_{3\text{pt},i}(\boldsymbol{q},t,t_s) = -ia^6 \sum_{\boldsymbol{x},\boldsymbol{y}} e^{i\boldsymbol{q}\cdot\boldsymbol{y}} \Gamma_{\beta\alpha} \left\langle O_{N,\alpha}(\boldsymbol{x},t_s)\, A^a_i(\boldsymbol{y},t)\, \overline{O}_{N,\beta}(0) \right\rangle$$

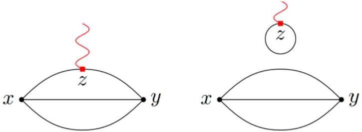

$$\left\{\begin{array}{l} u-d \\ u+d \\ u+d \end{array}\right. \longleftarrow \; = C^{a\,\boxed{\text{conn}}}_{3\text{pt,i}}(\boldsymbol{q},t,t_s) + C^{a\,\boxed{\text{disc}}}_{3\text{pt},i}(\boldsymbol{q},t,t_s) \longrightarrow \left\{\begin{array}{l} u+d-2s \\ u+d+s \end{array}\right.$$

with

$$C^{\text{disc}}_{3\text{pt},i}(\boldsymbol{q},t,t_s) = \left\langle L_i(\boldsymbol{q},t) C_2(\boldsymbol{p}',t_s) \right\rangle, \qquad L_i(\boldsymbol{q},t) = -\sum_{\boldsymbol{z}} e^{i\boldsymbol{q}\cdot\boldsymbol{z}} \mathrm{Tr}\left[\mathrm{D}_\mathrm{q}^{-1}(\mathrm{z},\mathrm{z})\gamma_\mathrm{i}\gamma_5\right]$$

- $\boldsymbol{p}' = \boldsymbol{0} \Rightarrow \boldsymbol{q} = -\boldsymbol{p}$, i.e. rest frame of the final state nucleon
- smeared u, d fields
- source-sink separation is $t_s = x_0 - y_0$

Ratio

The axial form factor G_A is addressed considering the transverse component $(\boldsymbol{q} \times \boldsymbol{A})$

$$C^{T}_{3\mathrm{pt},i}(\boldsymbol{q}, t, t_s) = \epsilon^{ijk} q_j \, C_{3\mathrm{pt},k}(\boldsymbol{q}, t, t_s) \propto (\boldsymbol{q} \times \boldsymbol{\gamma})_i \gamma_5 G_A(Q^2) + \cancel{(\boldsymbol{q} \times \boldsymbol{q})_i \gamma_5 G_P(Q^2)}$$

and then projecting into

$$C_{3\mathrm{pt}}(\boldsymbol{q}, t, t_s) = \sum_i \frac{(\boldsymbol{q} \times \boldsymbol{s})_i}{|\boldsymbol{q} \times \boldsymbol{s}|^2} C^{T}_{3\mathrm{pt},i}(\boldsymbol{q}, t, t_s) \,, \quad \boldsymbol{s} = \boldsymbol{e}_3 \,, \quad \Gamma = \frac{1}{2}(1 + \gamma_0)(1 + i\gamma_5\gamma_3)$$

The signal is improved considering only momenta $|q_3| \leq \min\left(|q_1|, |q_2|\right)$ and the ratio is

$$R(\boldsymbol{q}, t, t_s) = \frac{C_{3\mathrm{pt}}(\boldsymbol{q}, t, t_s)}{C_{2\mathrm{pt}}(\boldsymbol{0}, t_s)} \sqrt{\frac{C_{2\mathrm{pt}}(\boldsymbol{q}, t_s - t) C_{2\mathrm{pt}}(\boldsymbol{0}, t) C_{2\mathrm{pt}}(\boldsymbol{0}, t_s)}{C_{2\mathrm{pt}}(\boldsymbol{0}, t_s - t) C_{2\mathrm{pt}}(\boldsymbol{q}, t) C_{2\mathrm{pt}}(\boldsymbol{q}, t_s)}} \xrightarrow{t - t_s \gg 0} (\ldots) G_A^{\mathrm{eff}}(Q^2)$$

Channels and decomposition

We have three channels

$$(u-d) \qquad (u+d-2s) \qquad (u+d+s)$$

We focus on $(u+d+s)$ addressing isoscalar octet and strangeness separately

$$(u+d-2s)+3(s) \quad \Rightarrow \quad (u+d+s)$$

We can then obtain the flavour decomposition

$$\begin{aligned}
A^{u}_{\mu,R} &= \frac{1}{2}A^{u-d}_{\mu,R} + \frac{1}{6}A^{u+d-2s}_{\mu,R} + \frac{1}{3}A^{u+d+s}_{\mu,R}\,, \\
A^{d}_{\mu,R} &= -\frac{1}{2}A^{u-d}_{\mu,R} + \frac{1}{6}A^{u+d-2s}_{\mu,R} + \frac{1}{3}A^{u+d+s}_{\mu,R}\,, \\
A^{s}_{\mu,R} &= \frac{1}{3}\left[A^{u+d+s}_{\mu,R} - A^{u+d-2s}_{\mu,R}\right]\,,
\end{aligned}$$

NB: One option is also to perform the analysis on the flavour decomposed current

Channels and decomposition: signal

The signal is different for the 3 channels due to the different contributions of the disconnected data, which are noisier than the connected components.

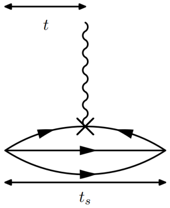

E300 (connected), $Q^2 = 0\,\mathrm{GeV}^2$

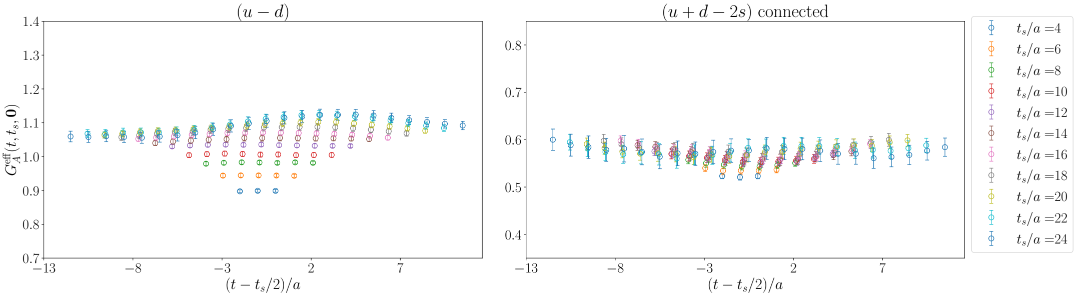

- small $t_s \Rightarrow$ small error, but high contamination from excited states
- large $t_s \Rightarrow$ large error, but small contamination from excited states

Channels and decomposition: signal

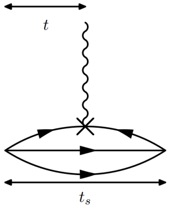

The signal is different for the 3 channels due to the different contributions of the disconnected data, which are noisier than the connected components.

E300 (disconnected), $Q^2 = 0\,\mathrm{GeV}^2$

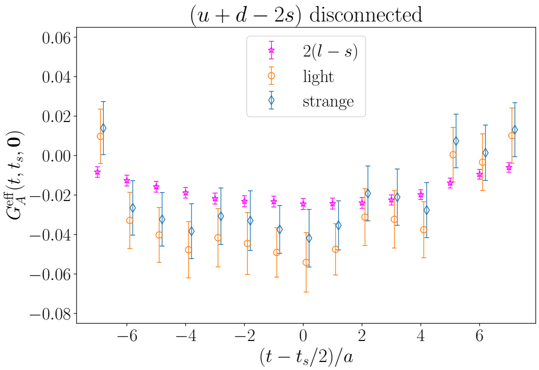

Channels and decomposition: signal

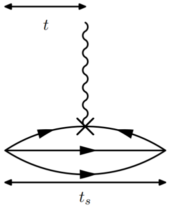

The signal is different for the 3 channels due to the different contributions of the disconnected data, which are noisier than the connected components.

E300 (connected+disconnected), $Q^2 = 0\,\mathrm{GeV}^2$

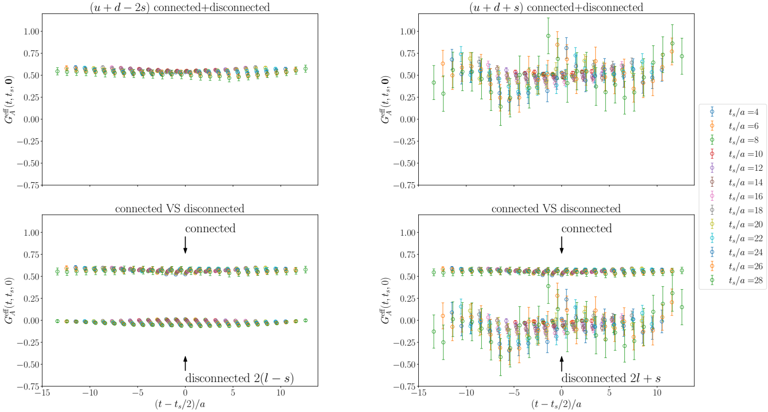

Analysis strategy

Analysis strategy (0)

There are different approaches to address the extraction of the relevant form factor:

- plateau method (**disconnected contributions**)
- summation method ($(u+d-2s)$ and **connected contribution**) [Maiani et al. (1987)[18], Capitani et al. (2012)[19]]

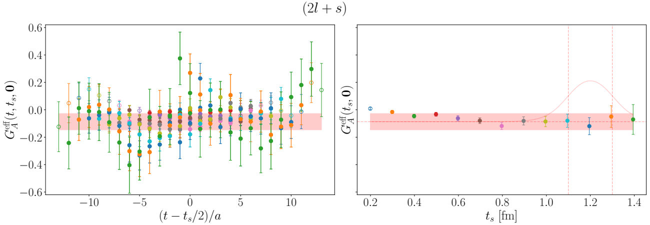

High level of statistical noise $\Rightarrow$ no detectable excited-state contamination within errors

Analysis strategy (0)

There are different approaches to address the extraction of the relevant form factor:

- plateau method (**disconnected contributions**)
- summation method ($(u+d-2s)$ and **connected contribution**) [Maiani et al. (1987)[18], Capitani et al. (2012)[19]]

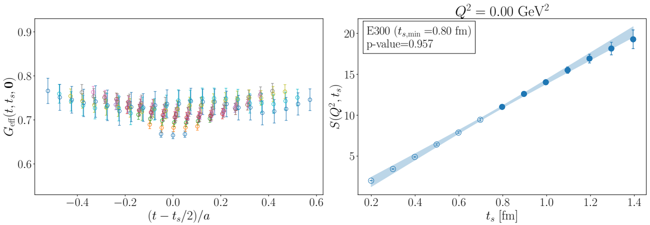

Excited states are suppressed exponentially with t_s instead of $t_s - t$:

$$S(\boldsymbol{q}, t_s) = a\sqrt{\frac{2E_q}{M_N + E_q}} \sum_{t=a}^{t_s - a} R(\boldsymbol{q}, t, t_s) \overset{t_s \gg 1}{=} b_0(\boldsymbol{q}) + t_s G_A(Q^2) + \mathcal{O}(t_s e^{-\Delta t_s})$$

Analysis strategy (1): connected (direct fit with z-expansion)

[Djukanovic et al. (2022)[10]]

We use z-expansion to parametrize the form factor ($n = 2$)

$$G_A(Q^2) = \sum_{k=0}^{n} a_k z^k(Q^2)\,, \quad z(Q^2) = \frac{\sqrt{t_{\mathrm{cut}} + Q^2} - \sqrt{t_{\mathrm{cut}}}}{\sqrt{t_{\mathrm{cut}} + Q^2} + \sqrt{t_{\mathrm{cut}}}}$$

Typical procedure (two-step fit) for every value of the $t_{s,\mathrm{min}}$:

1. for each Q^2, linear fit to $S(\boldsymbol{q}, t_s)$ for all point $t_s \in \{t_{s,\mathrm{min}}, \ldots\}$ to extract $G_A^{\mathrm{eff}}(Q^2, t_{s,\mathrm{min}})$
2. zfit in Q^2 range to extract a_0, a_1, a_2

HERE:

one-step **direct z-fit** on all data for all $t_s \in \{t_{s,\mathrm{min}}, \ldots\}$, $Q^2 \in \{0, \ldots, Q^2_{\mathrm{max}}\}$

$$t_{\mathrm{cut}} = (4M_\pi)^2\,, \qquad Q^2_{\mathrm{max}} = 0.7\,\mathrm{GeV}^2$$

Analysis strategy (1): connected (comparison of the approaches)

We compare three fit approaches

- two-step fit
- direct z-fit on G_A
- direct z-fit on both G_A and b_0

$$\sum_k^2 c_k z^k(Q^2)$$

$$S(Q^2, t_s) = \boxed{b_0(Q^2)} + t_s \boxed{G_A(Q^2)} \rightarrow \sum_k^2 a_k z^k(Q^2)$$

$$\{b_0(Q_1^2), b_0(Q_2^2), ..., b_0(Q_n^2)\}$$

$\Rightarrow$ all approaches are consistent!

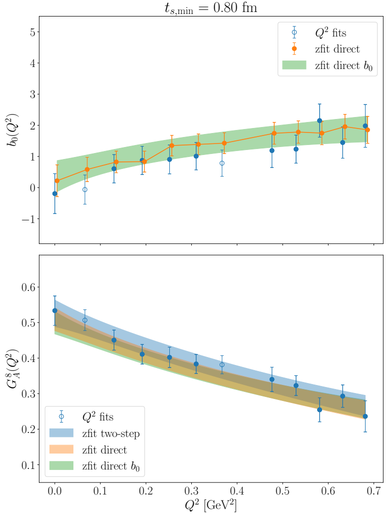

Analysis strategy (1): connected (window average)

We obtained in this way 3 coefficients of the z-expansion

$$a_0, a_1, a_2$$

We average over all the possible source-sink separation $t_{s,\mathrm{min}}$ with a window function

$$\frac{1}{N}\left[\tanh\left(\frac{t_s^{\mathrm{min}}-t_w^{\mathrm{low}}}{\Delta t_w}\right)-\tanh\left(\frac{t_s^{\mathrm{min}}-t_w^{\mathrm{up}}}{\Delta t_w}\right)\right]$$

$$\begin{cases} t_s^{\mathrm{low}} = 0.75\,\mathrm{fm} \\ t_s^{\mathrm{up}} = 0.95\,\mathrm{fm} \\ \Delta t_w = 0.08\,\mathrm{fm} \end{cases}$$

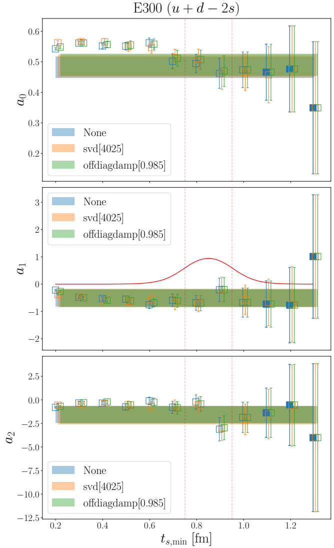

Analysis strategy (1): connected (window average)

We obtained in this way 3 coefficients of the z-expansion

We average over all t

$t_{s,\mathrm{min}}$ wi

$$\frac{1}{N}\left[\tanh\left(\frac{t_s^{\mathrm{min}} - \ldots}{\Delta t}\right.\right.$$

$$\begin{cases} t_s^{\mathrm{low}} = \ldots\ \mathrm{fm} \\ t_s^{\mathrm{up}} = 0.95\ \mathrm{fm} \\ \Delta t_w = 0.08\ \mathrm{fm} \end{cases}$$

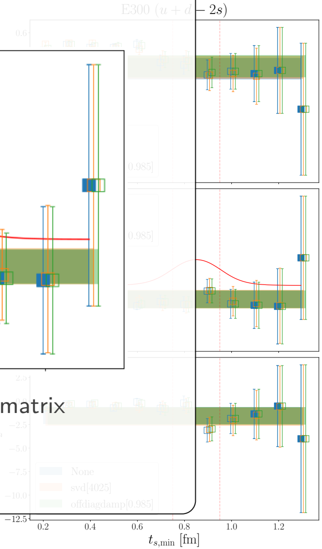

zoom on a_1

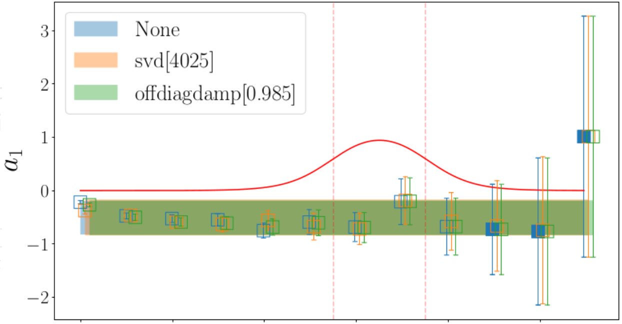

Legend: regularization of the covariance matrix

$\Rightarrow$ all approaches are compatible

Analysis strategy (2): disconnected

We use the **plateau method** + **window average** with $\begin{cases} t_s^{\text{low}} = 1.1\,\text{fm} \\ t_s^{\text{up}} = 1.3\,\text{fm} \\ \Delta t_w = 0.1\,\text{fm} \end{cases}$

- for every Q^2, perform plateau fits, then window average
- perform a z-fit on the resulting points

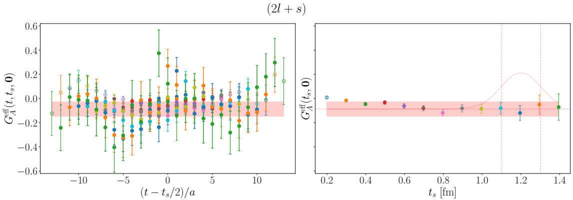

Analysis strategy (2): disconnected

We use the **plateau method** + **window average** with $\begin{cases} t_s^{\text{low}} = 1.1\,\text{fm} \\ t_s^{\text{up}} = 1.3\,\text{fm} \\ \Delta t_w = 0.1\,\text{fm} \end{cases}$ + **two-step z-fit**

- for every Q^2, perform plateau fits, then window average
- perform a z-fit on the resulting points

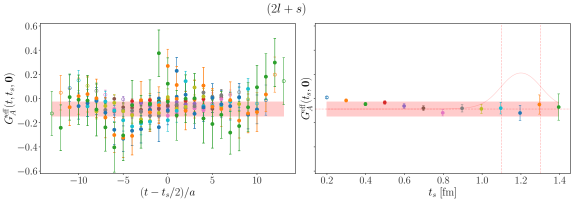

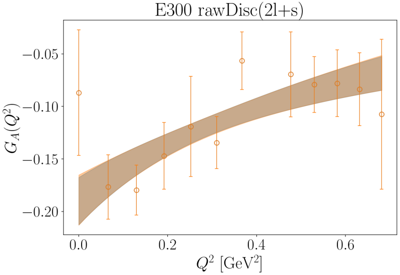

Analysis strategy (3): connected + disconnected

The final form factor is obtained combining the previous result

$$G_A(Q^2) = G_A^{\text{conn}}(Q^2) + G_A^{\text{disc}}(Q^2)$$

i.e. combining the coefficient of the z-expansion

Comparison with other approaches

- $(u + d + s) = (u + d - 2s) + 3s$
- $(u + d + s) = (u + d)$ (conn) + $(2l + s)$ (disc)

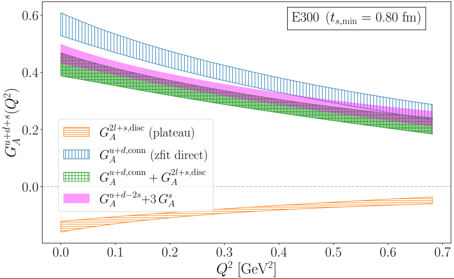

Chiral continuum extrapolation

General approach:

1. extract the z-expansion coefficients a_0, a_1, a_2 on all ensembles
2. extrapolate them to the chiral-continuum limit

Generally linear ansatz in M_π^2, a^2 for $a_i, i > 0$

$$a_i = p_0 + p_1 M_\pi^2 + s_0 a^2$$

and different ansatz for $a_0 \equiv g_A$ for depending on the channel, i.e.

- isovector: $a_0 = g_a^{(0)} + g_a^{(1)} M_\pi^2 + g_a^{(3)} M_\pi^3 - g_a^{(2)} M_\pi^2 \ln \frac{M_\pi}{M_N}$, with $g_a^{(k)}$ related from χPT
- isoscalar: same as a_i

We include FV term for the leading term a_0 for all channels

$$a_0 = (...) + v_0 \left(\frac{M_\pi^2}{\sqrt{M_\pi L}} e^{-M_\pi L} \right)$$

Chiral continuum extrapolation: example

[Barone et al. (2026)[4]]

Example of the **isoscalar singlet** $((u+d-2s)+3s)$ with FV term and cut in the coarsest lattice spacing

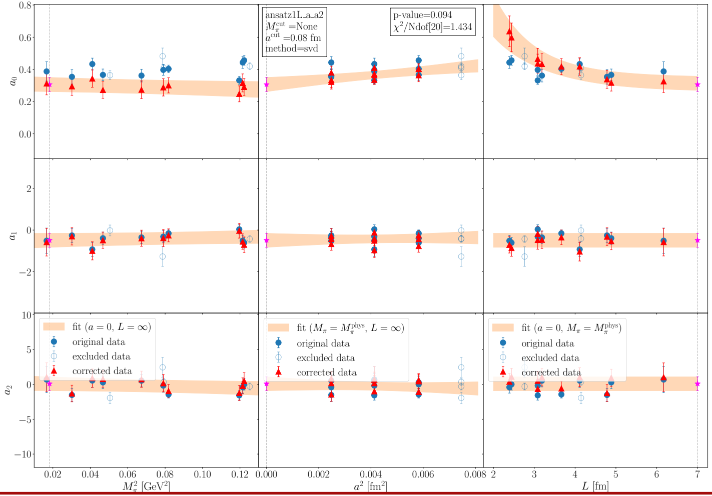

Model average: Akaike Information Criterion (AIC)

We assign AIC weights [Borsanyi et al. (2021)[20]] to all the fits as

weighted normal

$$w_{\boxed{k}}^{\mathrm{AIC}} \propto e^{-\frac{1}{2}(\chi_k^2 + 2n_{\mathrm{par},k} - n_{\mathrm{data},k})} \longrightarrow \boxed{P(a_i)} = \int_{-\infty}^{a_i} \sum_k \boxed{w_k^{\mathrm{AIC}} \mathcal{N}(a_i; \mu_k, \sqrt{\lambda}\sigma_k)}$$

$\forall$ fits

cumulative distribution function (CDF)

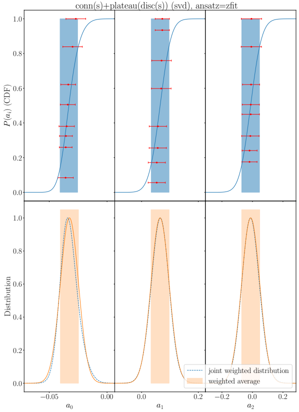

In practice here the distribution is gaussian, and we can equivalently use a simple weighted average

$$\langle x \rangle = \sum_k w_k^{\mathrm{AIC}} \langle x^{(k)} \rangle$$

which allows for a clean separation of statical/systematical error

$$\mathrm{Cov}^{\mathrm{stat}}[x^{(k)}, y^{(k)}] = \sum_k w_k^{\mathrm{AIC}} \mathrm{Cov}[x^{(k)}, y^{(k)}]$$

$$\mathrm{Cov}^{\mathrm{sys}}[x^{(k)}, y^{(k)}] = \sum_k w_k^{\mathrm{AIC}} \left[\langle x^{(k)} \rangle - \langle x \rangle\right] \left[\langle y^{(k)} \rangle - \langle y \rangle\right]$$

Results

Results

LQCD determination of the **nucleon axial structure** across flavor channels within a unified computational framework

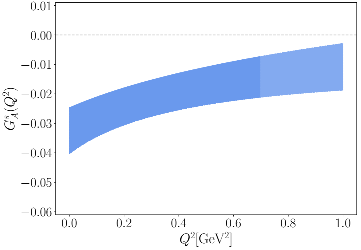

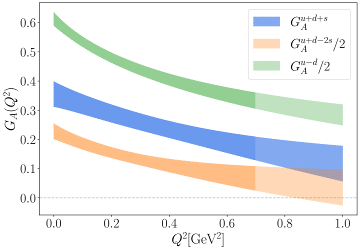

With charges

$$g_A^{u-d} = 1.225(46) \quad \text{[Djukanovic et al. (2022)[10]]}$$

$$g_A^{u+d-2s} = 0.457(40) \quad \text{[Barone et al. (2025)[3]]}$$

$$g_A^{u+d+s} = 0.355(43) \quad \text{[Barone et al. (2026)[4]]}$$

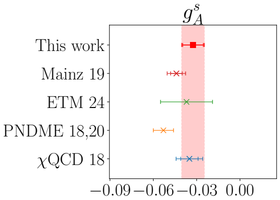

Outlook and conclusions

So far:

- full analysis of isovector $u - d$, isoscalar octet $u + d - 2s$ and singlet $u + d + s$
- singlet achieved through dedicated analysis of the strage s and disconnected diagrams
- analysis with summation method $+$ direct z-expansions at $n = 2$
- various approaches to regulate the covariance matrix all consistent ($\rightarrow$ svd)
- z-expansion coefficients evaluated on each ensemble and extrapolated to the continuum limit

Future work:

- refine the Q^2 spectrum of the disconnected contribution for better control
- determine the full flavour decomposition
- dedicated extraction of nucleon charges

THANK YOU!

Outlook and conclusions

So far:

- full analysis of isovector $u-d$, isoscalar octet $u+d-2s$ and singlet $u+d+s$
- singlet achieved through dedicated analysis of the strage s and disconnected diagrams
- analysis with summation method $+$ direct z-expansions at $n=2$
- various approaches to regulate the covariance matrix all consistent ($\rightarrow$ svd)
- z-expansion coefficients evaluated on each ensemble and extrapolated to the continuum limit

Future work:

- refine the Q^2 spectrum of the disconnected contribution for better control
- determine the full flavour decomposition
- dedicated extraction of nucleon charges

THANK YOU!

References I

[1] A. S. Meyer et al., "Status of Lattice QCD Determination of Nucleon Form Factors and their Relevance for the Few-GeV Neutrino Program", Ann. Rev. Nucl. Part. Sci. **72**, 205–232 (2022), arXiv:2201.01839 [hep-lat].

[2] A. S. Meyer et al., "Deuterium target data for precision neutrino-nucleus cross sections", Phys. Rev. D **93**, 113015 (2016), arXiv:1603.03048 [hep-ph].

[3] A. Barone et al., "Isoscalar octet axial form factor of the nucleon from lattice QCD", Phys. Rev. D **112**, 014503 (2025), arXiv:2503.18848 [hep-lat].

[4] A. Barone et al., "The strange and flavor-singlet axial form factors of the nucleon from lattice QCD", (2026), arXiv:2605.06559 [hep-lat].

[5] C. Alexandrou et al., "Quark flavor decomposition of the nucleon axial form factors", Phys. Rev. D **104**, 074503 (2021), arXiv:2106.13468 [hep-lat].

[6] X.-D. Ji, "Gauge-Invariant Decomposition of Nucleon Spin", Phys. Rev. Lett. **78**, 610–613 (1997), arXiv:hep-ph/9603249.

[7] V. Y. Alexakhin et al., "The Deuteron Spin-dependent Structure Function g1(d) and its First Moment", Phys. Lett. B **647**, 8–17 (2007), arXiv:hep-ex/0609038.

[8] T. Miceli et al., "Improving Dark Matter Searches by Measuring the Nucleon Axial Form Factor: Perspectives from MicroBooNE", Phys. Procedia **61**, edited by F. Avignone and W. Haxton, 495–501 (2015), arXiv:1406.5204 [hep-ex].

References II

[9] K. S. Kim et al., "Role of axial mass and strange axial form factor from various target nuclei in neutrino-nucleus scattering", Phys. Rev. C **100**, 034604 (2019).

[10] D. Djukanovic et al., "Isovector axial form factor of the nucleon from lattice QCD", Phys. Rev. D **106**, 074503 (2022), arXiv:2207.03440 [hep-lat].

[11] D. Djukanovic et al., "Electromagnetic form factors of the nucleon from Nf=2+1 lattice QCD", Phys. Rev. D **109**, 094510 (2024), arXiv:2309.06590 [hep-lat].

[12] D. Djukanovic et al., "Precision Calculation of the Electromagnetic Radii of the Proton and Neutron from Lattice QCD", Phys. Rev. Lett. **132**, 211901 (2024), arXiv:2309.07491 [hep-lat].

[13] D. Djukanovic et al., "Zemach and Friar radii of the proton and neutron from lattice QCD", Phys. Rev. D **110**, L011503 (2024), arXiv:2309.17232 [hep-lat].

[14] B. Sheikholeslami and R. Wohlert, "Improved Continuum Limit Lattice Action for QCD with Wilson Fermions", Nucl. Phys. B **259**, 572 (1985).

[15] J. Bulava and S. Schaefer, "Improvement of $N_f = 3$ lattice QCD with Wilson fermions and tree-level improved gauge action", Nucl. Phys. B **874**, 188–197 (2013), arXiv:1304.7093 [hep-lat].

[16] M. Luscher and P. Weisz, "On-shell improved lattice gauge theories", Commun. Math. Phys. **98**, [Erratum: Commun.Math.Phys. 98, 433 (1985)], 433 (1985).

[17] M. Bruno et al., "Simulation of QCD with $\mathrm{N}_f = 2 + 1$ flavors of non-perturbatively improved Wilson fermions", JHEP **02**, 043 (2015), arXiv:1411.3982 [hep-lat].

References III

[18] L. Maiani et al., "Scalar Densities and Baryon Mass Differences in Lattice QCD With Wilson Fermions", Nucl. Phys. B **293**, 420 (1987).

[19] S. Capitani et al., "The nucleon axial charge from lattice QCD with controlled errors", Phys. Rev. D **86**, 074502 (2012), arXiv:1205.0180 [hep-lat].

[20] S. Borsanyi et al., "Leading hadronic contribution to the muon magnetic moment from lattice QCD", Nature **593**, 51–55 (2021), arXiv:2002.12347 [hep-lat].

Backup

BACKUP

Dealing with a large covariance matrix

Direct z-fit

- PRO: do only one fit and account for everything in one step
- CON: for small $t_{s,\mathrm{min}}$ the covariance matrix $C_{N\times N}$ is **large** with $N = (\#Q^2) \times (\#t_s)$ and possibly not optimally estimated ($\equiv$ error on the error is large)

To assess the stability of the fits we estimate the covariance of the data y with

- standard
- shrinkage (off-diagonal damping with a parameter $\alpha \in [0.985, 1]$, i.e. up to 1.5% damping)
- SVD cut (reduce the condition number of the matrix)

$$C_{ij} = \langle (y_i - \langle y_i \rangle)(y_j - \langle y_j \rangle) \rangle$$

Dealing with a large covariance matrix

Direct z-fit

- PRO: do only one fit and account for everything in one step
- CON: for small $t_{s,\min}$ the covariance matrix $C_{N\times N}$ is **large** with $N = (\#Q^2) \times (\#t_s)$ and possibly not optimally estimated ($\equiv$ error on the error is large)

To assess the stability of the fits we estimate the covariance of the data y with

- standard
- shrinkage (off-diagonal damping with a parameter $\alpha \in [0.985, 1]$, i.e. up to 1.5% damping)
- $\boxed{\text{SVD cut}}$ (reduce the condition number of the matrix)

$$C_{ij} = \langle (y_i - \langle y_i \rangle)(y_j - \langle y_j \rangle) \rangle$$

$$C^s_{ij} = (1-\alpha)\delta_{ij} C_{ij} + \alpha C_{ij}$$

Dealing with a large covariance matrix

Direct z-fit

- PRO: do only one fit and account for everything in one step
- CON: for small $t_{s,\mathrm{min}}$ the covariance matrix $C_{N\times N}$ is **large** with $N = (\#Q^2) \times (\#t_s)$ and possibly not optimally estimated ($\equiv$ error on the error is large)

To assess the stability of the fits we estimate the covariance of the data y with

- standard
- shrinkage (off-diagonal damping with a parameter $\alpha \in [0.985, 1]$, i.e. up to 1.5% damping)
- $\boxed{\text{SVD cut}}$ (reduce the condition number of the matrix)

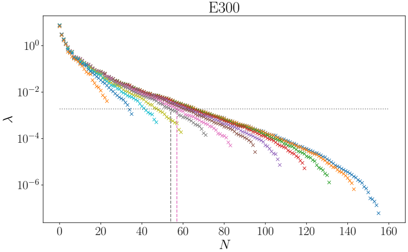

Strategy: scan progressively removing the lowest eigenvalues (setting them constant), stop when the χ^2 of the fit is acceptable.
Set set same condition number for all the $t_{s,\mathrm{min}}$

From the path integral to a numerical problem

We move to Euclidean space through **Wick rotation** $t \to -i\tau$. The path integral becomes

$$\langle \mathcal{O} \rangle = \frac{1}{Z} \int \mathcal{D}[\Phi] \mathcal{O}[\Phi] \, e^{iS_M[\Phi]} \quad \Rightarrow \quad \langle \mathcal{O} \rangle = \frac{1}{Z} \int \mathcal{D}[\Phi] \mathcal{O}[\Phi] \, e^{-S_E[\Phi]} , \quad \Phi = (\bar{\psi}, \psi, U)$$

We can now interpret the exponential as a **Boltzmann factor** (with real S_E)! After integrating out the fermion fields, we can then use **Monte Carlo** to evaluate multidimensional integrals by generating a large number of gauge configurations U_α with probability

$$P[U_\alpha] \propto \det[U_\alpha] e^{-S_E[U_\alpha]}$$

and estimate the path integral as

$$\langle \mathcal{O} \rangle \simeq \frac{1}{N_{\text{config}}} \sum_{\alpha=1}^{N_{\text{config}}} \mathcal{O}[U_\alpha]$$

Correlation functions: the fundamental lattice observables

The basic quantities computed on the lattice are Euclidean correlation functions, e.g.

$$C_2(t) = \sum_{\boldsymbol{x}} \langle 0 | O_{B_s}(\boldsymbol{x}, t)\, O^\dagger_{B_s}(\boldsymbol{0}, 0) | 0 \rangle \qquad O_{B_s}(x) = \bar{b}(x)\gamma_5 s(x)$$

The correlator has the **spectral decomposition**

$$C_2(t) = \int_0^\infty \mathrm{d}\omega \rho(\omega) e^{-\omega t} = \sum_n |\langle 0 | O_{B_s} | n \rangle|^2 e^{-E_n t}.$$

with a **discrete spectral density**

$$\rho(\omega) = \sum |\langle 0 | O_{B_s} | n \rangle|^2 \delta(\omega - E_n)$$

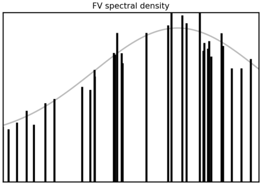

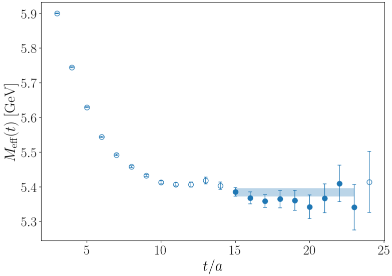

$$C_2(t) \xrightarrow{t \gg 0} |Z_0|^2 e^{-E_0 t}$$

$$M_{\mathrm{eff}}(t) = -\log\left(\frac{C_2(t+1)}{C_2(t)}\right)$$

Computational pipeline

Monte Carlo gauge ensembles → Correlation functions → Statistical analysis → Physics observables

1. Large-scale computing for ensemble generation and measurements on HPC (C/C++)

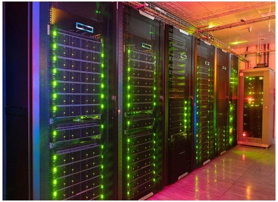

2. Preprocessing Euclidean correlation functions (large datasets generated on multiple gauge ensembles with different properties and parameters)
3. Data analysis (Python): error propagation, fits, extrapolations, uncertainty quantification